PNAS RESEARCH ARTICLE | IMMUNOLOGY AND INFLAMMATION

Platelet-activating factor (PAF) promotes immunosuppressive neutrophil differentiation within tumors

Ankit Dahal[a], Yeonsun Hong[a], Jocelyn S. Mathew[a], Adam Geber[a], Sarah Eckl[a], Stephanie Renner[a], Cooper J. Sailer[b], Allison T. Ryan[a], Sana Mir[a], Kihong Lim[a], David C. Linehan[c,d], Scott A. Gerber[a,c,d], and Minsoo Kim[a,c,1]

Affiliations are included on p. 10.

Edited by Gabriel Rabinovich, Universidad de Buenos Aires, Buenos Aires CABA, Argentina; received April 3, 2024; accepted July 8, 2024

Chronic inflammatory milieu in the tumor microenvironment (TME) leads to the recruitment and differentiation of myeloid-derived suppressor cells (MDSCs). Polymorphonuclear (PMN)-MDSCs, which are phenotypically and morphologically defined as a subset of neutrophils, cause major immune suppression in the TME, posing a significant challenge in the development of effective immunotherapies. Despite recent advances in our understanding of PMN-MDSC functions, the mechanism that gives rise to immunosuppressive neutrophils within the TME remains elusive. Both in vivo and in vitro, newly recruited neutrophils into the tumor sites remained activated and highly motile for several days and developed immunosuppressive phenotypes, as indicated by increased arginase 1 (Arg1) and dcTrail-R1 expression and suppressed anticancer CD8 T cell cytotoxicity. The strong suppressive function was successfully recapitulated by incubating naive neutrophils with cancer cell culture supernatant in vitro. Cancer metabolite secretome analyses of the culture supernatant revealed that both murine and human cancers released lipid mediators to induce the differentiation of immunosuppressive neutrophils. Liquid chromatography–mass spectrometry (LC-MS) lipidomic analysis identified platelet-activation factor (PAF; 1-*O*-alkyl-2-acetyl-*sn*-glycero-3-phosphocholine) as a common tumor-derived lipid mediator that induces neutrophil differentiation. Lysophosphatidylcholine acyltransferase 2 (LPCAT2), the PAF biosynthetic enzyme, is up-regulated in human pancreatic ductal adenocarcinoma (PDAC) and shows an unfavorable correlation with patient survival across multiple cancer types. Our study identifies PAF as a lipid-driven mechanism of MDSC differentiation in the TME, providing a potential target for cancer immunotherapy.

tumor microenvironment | MDSC | neutrophil | Cancer | myeloid cells

Significance

Myeloid-derived suppressor cells (MDSCs) are major "pro-tumorigenic" cells of the tumor microenvironment that support cancer development and hamper antitumor host immune response. Although MDSCs are a heterogeneous group of cells, polymorphonuclear (PMN)-MDSCs, which are phenotypically and morphologically similar to neutrophils, play a major role in adverse clinical outcomes. This suggests that the presence of PMN-MDSCs is an important prognostic biomarker and rational target for therapeutic blockade. Despite recent advances, our understanding of the underlying molecular mechanisms by which classical neutrophils differentiate into PMN-MDSC within the tumor microenvironment remains largely unknown. Our study identifies platelet-activation factor (PAF) as a lipid-driven mechanism of MDSC differentiation in the tumor microenvironment, providing a potential target for cancer immunotherapy.

The dynamic interaction between cancer and immune cells within the tumor microenvironment (TME) confers major mechanisms of anticancer immune evasion, including the differentiation of myeloid cells into highly immunosuppressive cells termed myeloid-derived suppressor cells (MDSCs) (1). Although MDSCs are a heterogeneous group of cells that captures all immunosuppressive myeloid populations, polymorphonuclear (PMN)-MDSCs, which are phenotypically and morphologically similar to neutrophils, make up a substantial portion of MDSCs (2). The presence of neutrophils within the TME is associated with significant mortality and morbidity for cancer patients (3–8), suggesting that PMN-MDSCs are important prognostic biomarkers and rational targets for therapeutic blockade.

Chronic inflammatory and immunomodulatory signals within the TME lead to both the recruitment and differentiation of neutrophils into MDSCs (9–11). Despite these advances in our understanding of PMN-MDSC biology, comprehensive profiling of the inflammatory tumor milieus and the key molecular regulators of MDSC differentiation are incompletely understood. Here, we sought to systematically identify the molecular mediators that promote immunosuppressive neutrophil phenotype in murine and human cancers.

Bioactive, metabolic derivatives of membrane phospholipids such as prostaglandins, leukotrienes, lipoxins, and platelet-activating factor serve as potent neutrophil activators and regulators of local inflammatory responses (12). Prostaglandin E2 (PGE2) has canonically been characterized as a chemotactic and inflammatory signal; however, increasing evidence suggests that PGE2 can also modulate neutrophil intrinsic anti-inflammatory and proangiogenic responses at sites of tissue injury during wound healing and cancer (13–16). In addition, the lipid metabolism of cancer cells is altered, in part, to enhance cellular membrane synthesis to support cell proliferation and survival and to promote inflammation within the TME (17). Consequently, the accumulation of lipids such as PGE2, cholesterols, and short-chain fatty acids limits anticancer immune responses (18). The PGE2-EP2/EP4 receptor axis in MDSC differentiation has been implicated in the

Author contributions: A.D. and M.K. designed research; A.D., Y.H., J.S.M., S.E., S.R., C.J.S., A.T.R., S.M., and K.L. performed research; D.C.L. and S.A.G. contributed new reagents/analytic tools; A.D., Y.H., A.G., C.J.S., A.T.R., S.M., and K.L. analyzed data; and A.D. and M.K. wrote the paper.

The authors declare no competing interest.

This article is a PNAS Direct Submission.

[1]To whom correspondence may be addressed. Email: minsoo_kim@urmc.rochester.edu.

This article contains supporting information online at https://www.pnas.org/lookup/suppl/doi:10.1073/pnas.2406748121/-/DCSupplemental.

Published August 23, 2024.

pathogenesis of multiple cancers (19). However, multiple findings also point to other lipid and protein-mediated mechanisms of MDSC differentiation, suggesting that an array of cancer-secreted molecular mediators likely play a role in the establishment of an immunosuppressive TME (20, 21). A comprehensive investigation of such cancer-derived bioactive molecules in mediating MDSC differentiation across different cancer types is largely incomplete.

Here, we found that cancer-secreted factors in vitro are sufficient to promote the differentiation of naive neutrophils into MDSCs that transcriptionally and phenotypically mirror the immunosuppressive subset of neutrophils present within the TME of murine and human cancers. Profiling of the cancer metabolite secretome demonstrated that both murine and human cancers released lipid mediators to induce MDSC differentiation. We further identified a common tumor-derived lipid mediator that induces neutrophil differentiation: platelet-activation factor (PAF; 1-*O*-alkyl-2-acetyl-*sn*-glycero-3-phosphocholine). Our findings reveal a mechanism of MDSC differentiation that provides a potential therapeutic target for enhancing immunotherapeutic response in PDAC and other cancers.

Results

Interaction of Cancer Cells and Neutrophils Dictates the Mechanism of PMN-MDSC Differentiation. To investigate the mechanism of MDSC differentiation, we first established an orthotopic KCKO murine pancreatic ductal adenocarcinoma (PDAC) model (22). We harvested neutrophils from the bone marrow, spleen, and the tumor at days 7 and 14 post tumor inoculation. Flow cytometry and intravital imaging demonstrated growing numbers of neutrophils and T cells within the TME, similar to those observed in human disease (Fig. 1*A* and *SI Appendix*, S1*A*) (3, 23–25). Interestingly, only the neutrophils isolated from the tumor exhibited immunosuppressive function, as measured by the expression of MDSC markers, including arginase (Arg1) and dcTrail-R1 (Fig. 1 *B*–*D*), and the ability to inhibit T cell proliferation (Fig. 1 *E* and *F*) (24–28). This suggests that

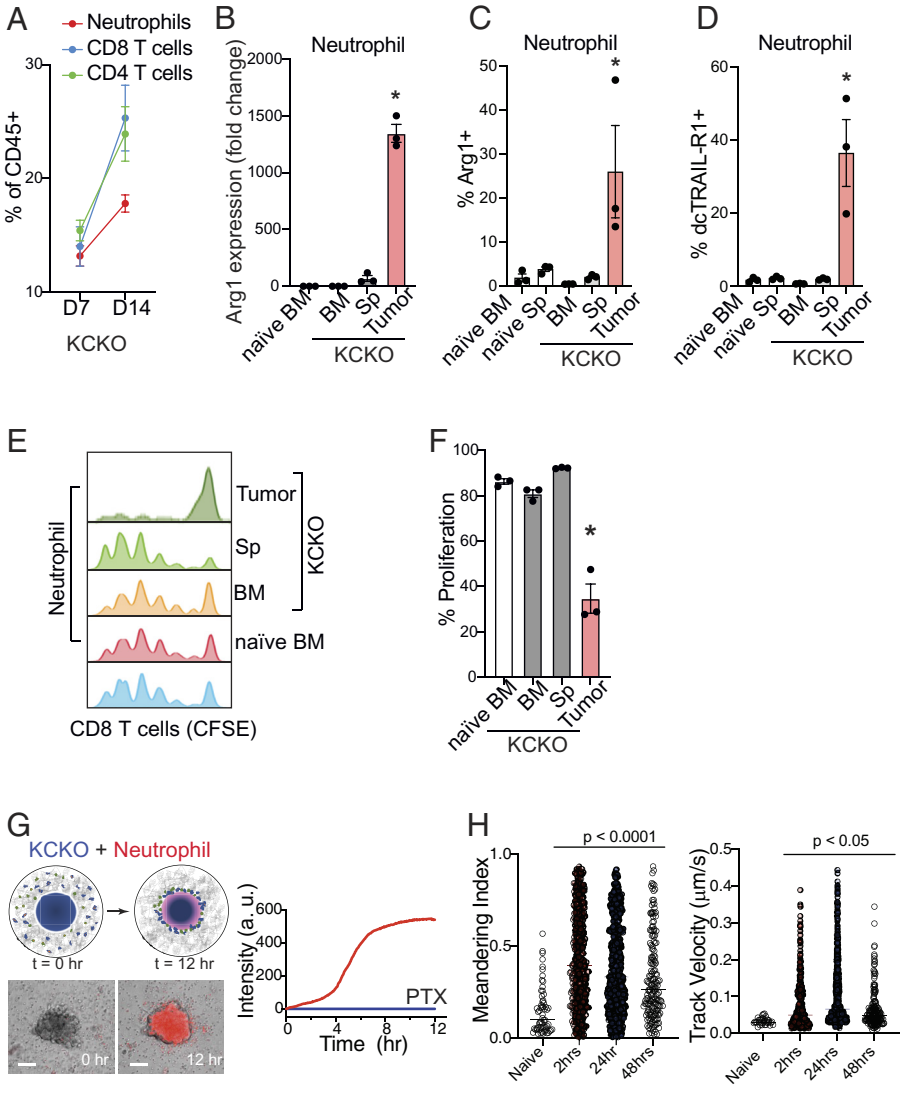

Fig. 1. Cancer cell–neutrophil interaction directly regulates PMN-MDSC differentiation. (*A*) Neutrophils, CD8, and CD4 T cells were isolated from orthotopic KCKO tumors, and relative abundance of each cell type was quantified using flow cytometry. (*B*) qPCR and flow cytometric quantification of (*C*) Arginase 1 and (*D*) dcTRAIL-R1 expression in neutrophils isolated from different organs of naïve and tumor-bearing mice. (*E* and *F*) Neutrophils isolated from different organs were cocultured with CFSE-labeled CD8 T cells to assess neutrophil-mediated suppression of T cell proliferation. (*G*) Schematic of neutrophil migration into KCKO tumoroid. Images from 0 h and 12 h after incubation are shown. The graph depicts the MFI of neutrophils that migrated into the KCKO tumoroid (Red). Neutrophil migration kinetics after adding Pertussis Toxin (PTX) is shown in blue. (*H*) The meandering index and track velocity of neutrophils cultured with cancer cells were calculated at different time points after incubation with KCKO cancer. Data from (*B*), (*C*), and (*F*) include n = 3, $P < 0.0001$, and (*D*) n = 3, $P < 0.05$ as determined by the one-way ANOVA test with Tukey's multiple-comparison post hoc test. (*H*) One-way ANOVA test with Tukey MCT.

a microenvironmental cue that mediates MDSC differentiation may be localized to the TME.

Based on our finding, we hypothesized that direct cancer cell–neutrophil interactions may be necessary for MDSC differentiation within the TME. To address this, we established a 3D in vitro tumor spheroid-neutrophil coculture system for live cell imaging using KCKO and E0771 cancer cells and naive neutrophils isolated from the bone marrow (Movie S1). Live neutrophil migration images with the tumor spheroids showed that neutrophils were immediately drawn toward cancer cells, dramatically swarming into the tumoroid region, and remained highly motile for up to 12 h (Fig. 1*G* and *SI Appendix*, S1*B*). Additionally, neutrophils isolated from both naïve and tumor-bearing mice spleens showed similar cell migration kinetics into the tumor spheroids, further suggesting that the local inflammatory TME is the major driver of neutrophil migration and activation (Movie S2 and *SI Appendix*, S1*C*). To further investigate this phenomenon, we imaged neutrophil–cancer interactions in a 2D setting and quantified neutrophil motility by measuring neutrophil meandering index and by tracking velocity up to day 2 post-inoculation (Fig. 1*H*). Surprisingly, neutrophils stayed active for more than 48 h. Additionally, these long-lived neutrophils (approximately 10% of seeded neutrophils) morphologically continued to increase in size to day 5 and remained motile (*SI Appendix*, S1 *D* and *E* and Movie S3). These data suggest that cancer cells can directly recruit neutrophils into the TME and induce a unique phenotypic reprogramming to activate and promote extended survival in neutrophils.

Given the prolonged survival and active migration of neutrophils in the tumor spheroids in vitro, we hypothesized that cancer-secreted factors may directly mediate the neutrophil activation. To test this hypothesis, we cultured bone marrow isolated neutrophils with KCKO cell supernatant overnight. The incubation of naïve neutrophils with cancer supernatants significantly increased the expression of neutrophil activation markers, including the upregulation of cell surface marker CD11b (29) and the downregulation of CD62L (30) (Fig. 2*A*). We further found that cancer-secreted factors in the supernatants increased the lifespan of neutrophils, which exhibited a half-life of 3 d (Fig. 2*B* and *SI Appendix*, S2*A*), and were sufficient to promote MDSC differentiation, as measured by the substantial increase in Arg1 induction (Fig. 2*C*). To investigate whether this change is also observed in vivo, we used interstitial fluid directly isolated from orthotopic KCKO tumors and cultured with naïve, bone marrow–derived neutrophils. Importantly, we used interstitial fluid isolated from a healthy (non-tumor-bearing) pancreas as a negative control. Consistent with the in vitro culture supernatant, the neutrophils cultured with in vivo tumor interstitial fluid exhibited extended survival, activation, and MDSC differentiation (dcTRAIL-R1 expression) (Fig. 2*D*). Additionally, neutrophils pulsed with cancer supernatants showed significant inhibition of T cell proliferation and anticancer T cell cytotoxicity in both KCKO and E0771

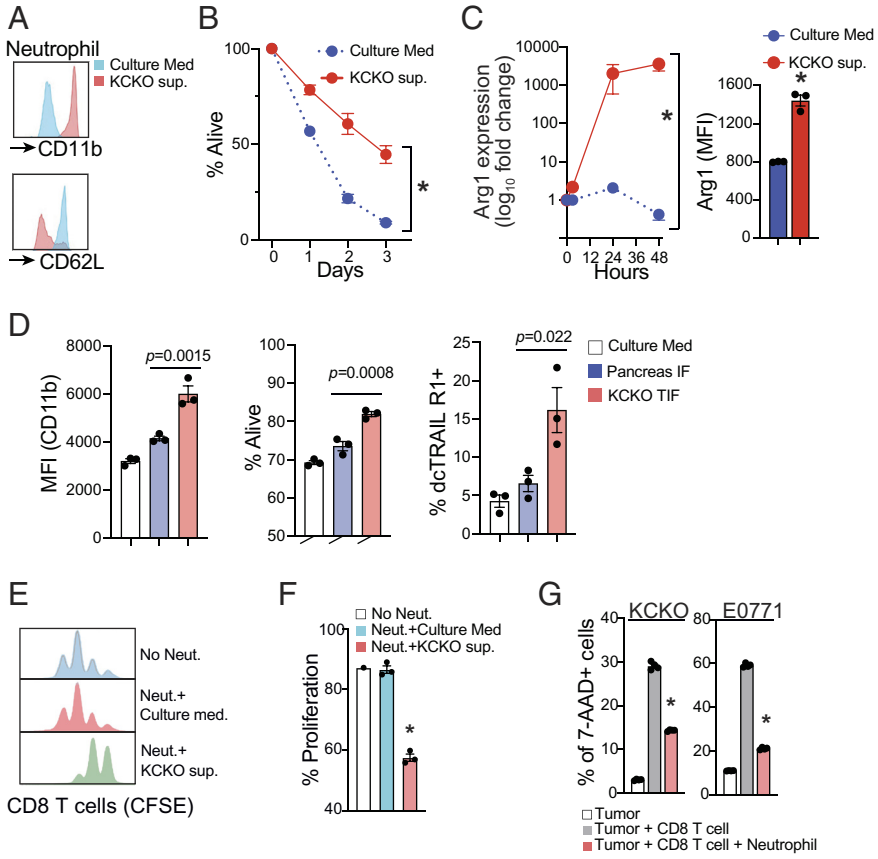

Fig. 2. Cancer-secreted factors promote PMN-MDSC differentiation in vitro. (*A*) MFI of neutrophil activation markers CD11b and CD62L was quantified using flow cytometry. (*B*) Neutrophil survival was measured at different time points using flow cytometry to count the number of live neutrophils present in the culture at each day. (*C*) Arg1 expression was quantified at different time points after neutrophils were cultured in KCKO cancer supernatant using qPCR for RNA and flow cytometry for Arg1 protein expression after 24 h in culture. (*D*) Naïve neutrophils were cultured either in culture media or media containing pancreatic interstitial fluid or tumor interstitial fluids for 18 h. Neutrophil activation (CD11b), percent alive, and percent dcTRAIL-R1 positive are quantified. (*E* and *F*) Suppression of CD8 T cell proliferation. (*G*) OT1 T cells were cocultured with OVA-pulsed KCKO or E0771 cancer cells in the presence of cancer supernatant pulsed neutrophils. Cytotoxicity was quantified using flow cytometric reading for 7AAD-positive cancer cells. (*A*) n = 3. (*B* and *C*) Ordinary two-way ANOVA test, n = 3, $P < 0.0001$. (*D*) n = 3, one-way ANOVA, Tukey's MCT. (*F*) Student's *t* test, $P < 0.0001$. (*G*) One-way ANOVA test, n = 3, Tukey's MCT, $P < 0.01$.

cancer cells (Fig. 2 *E*–*G*). Other canonical forms of PMN activators, such as LPS and TNFα, did not have the same response (*SI Appendix*, S2 *B* and *C*). Our data further support that cancer-secreted factors are highly localized to the TME and are sufficient to recruit neutrophils to the tumor and promote their differentiation into immunosuppressive cells.

A recent publication highlighted that tumor-associated neutrophils (TANs) are phenotypically diverse, revealing a continuum of three neutrophil subsets, including inflammatory (defined as T1 and T2) and immunosuppressive subsets (defined as T3) (26). Using RNA sequencing, we demonstrated that in vitro differentiation of neutrophils with cancer supernatants uniquely recapitulated the immunosuppressive, T3, subset of TANs by 1 d in culture and progressively expressed higher T3 gene signatures at day 2, suggesting that the in vitro stimulation by cancer-secreted factors was sufficient to promote immunosuppressive features of neutrophils that resemble the in vivo differentiation within the tumor (S2D).

Cancer-Secreted Factors Promote MDSC Differentiation in Murine and Human Neutrophils Across Multiple Cancer Types

To determine whether the cancer-secreted factors that promote PMN-MDSC differentiation are conserved in other cancer types, we tested multiple murine cancers including MC38 (colorectal) and E0771 (breast) cancer cell lines. Similar to KCKO culture supernatant, culture supernatant from all other cancer cell lines successfully promoted sustained neutrophil activation as observed by increased CD11b expression (Fig. 3*A*) and survival (Fig. 3*B*),

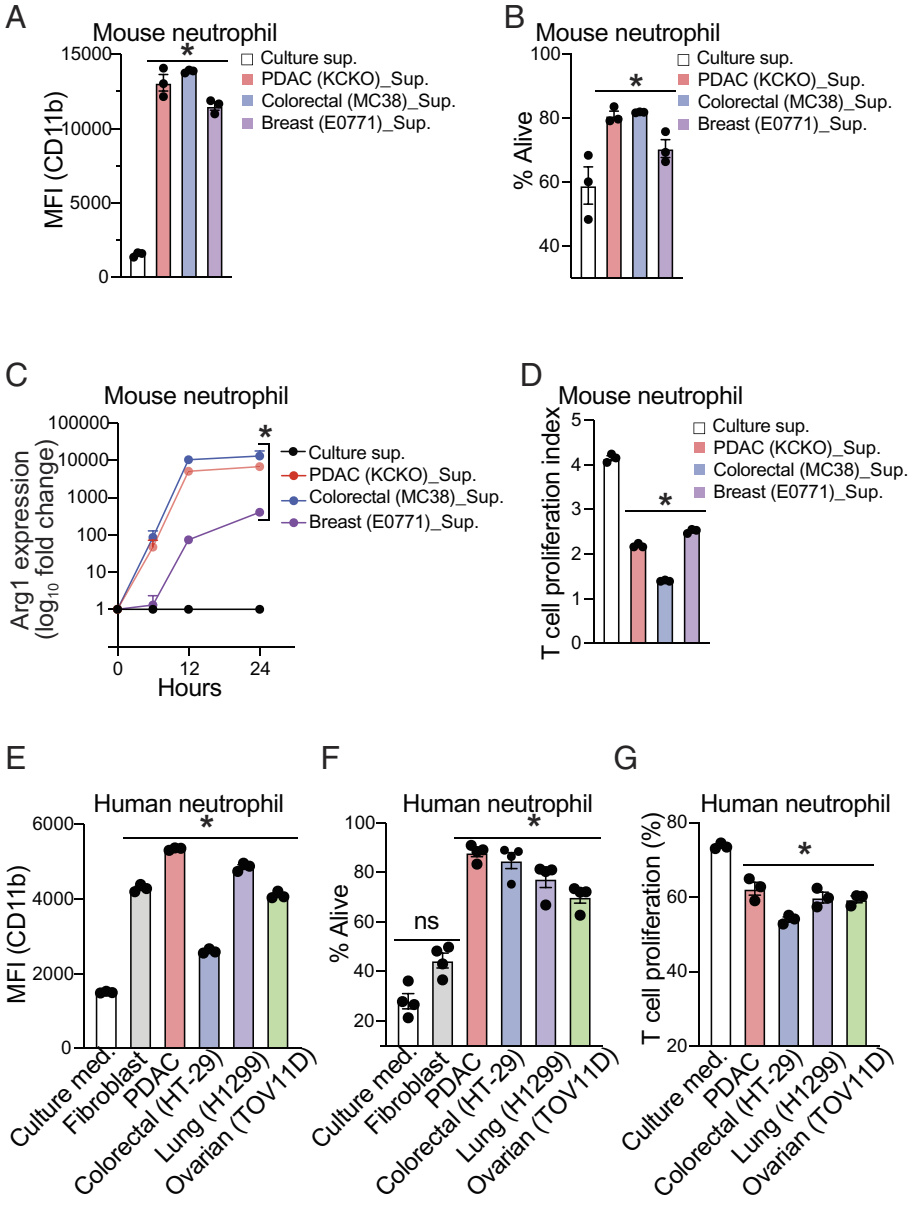

Fig. 3. Cancer-secreted factors promote MDSC differentiation in murine and human neutrophils across multiple cancer types. (*A* and *B*) Neutrophil activation (*A*) and survival (*B*) across different cancer supernatants after 12 h in culture were quantified using MFI of CD11b expression and Annexin V staining, respectively. (*C*) Kinetics of Arg1 expression quantifying expression across the various murine cancer types up to 24 h in culture. (*D*) CD8 T cell proliferation index (the average number of divisions of proliferating cells) after overnight coculture with cancer-supernatant conditioned neutrophils. (*E* and *F*) Activation (*E*) and survival (*F*) of human neutrophils after coculturing with supernatants prepared from human cancers or cancer-associated fibroblast. (*G*) Human CD8 T cell proliferation after being cocultured with cancer supernatant-conditioned human neutrophils for 3 d. Data from *A*, *B*, *C*, *D*, *E*, *F*, *G*, and *H*: n = 3, one-way ANOVA, Tukey's MCT. *C*: n = 3, two-way ANOVA, $P < 0.001$.

and increased Arg1 expression (Fig. 3*C*) and the ability to inhibit T cell proliferation (Fig. 3*D* and *SI Appendix*, S3*A*). To test whether this phenomenon is also conserved in human cancer cells, we cultured primary human neutrophils isolated from the blood of healthy donors with cancer supernatants from various human cancer cell lines, including PDAC3 (primary pancreatic cancer), HT-29 (colorectal cancer), H1299 (lung cancer), TOV11D (ovarian cancer) cell lines. We also used cancer-associated fibroblasts (CAF) isolated from human PDAC as a noncancer control. Similar to the murine data, human neutrophils in cancer supernatants exhibited enhanced activation, increased survival, and limited T cell proliferation as compared to neutrophils in normal culture media (Fig. 3 *E*–*G* and *SI Appendix*, S3 *B*–*D*). Neutrophils cultured with CAF supernatant also exhibited slightly increased activation and survival compared to the culture media conditions, but the extent of their survival capacity was significantly lower than that of the cancer cell lines, suggesting that the signals that promote neutrophil survival and MDSC differentiation are primarily driven by cancer cells.

Selective Depletion of Cancer-Secreted Lipid Mediators Abrogates PMN-MDSC Differentiation in Both Murine and Human Cancers. Certain cytokines such as GM-CSF, M-CSF, G-CSF, and SCF can be directly secreted by cancer cells and impact neutrophil differentiation (31–34). Therefore, we next sought to profile the cancer-secreted factors (cytokines and/or growth factors) mediating conserved MDSC differentiation across various human and murine cancer types. We performed a protein array of KCKO cell supernatants and identified major cancer-secreted proteins in the culture supernatants, including CCL2, CCL5, CCL9, CCL20, and osteopontin (OPN) (S4A). To determine whether these protein factors induce MDSC differentiation, we irreversibly denatured these proteins in the cancer supernatant by heat-inactivation (35). Interestingly, the heat inactivation did not alter neutrophil activation and dcTrail-R1 expression by the cancer supernatant (Fig. 4 *A*–*C*), while Arg1 expression and neutrophil survival were slightly increased (Fig. 4*B* and *SI Appendix*, S4*B*). Denatured proteins have been considered as one of the major inflammatory mediators (36). Thus, heat-induced protein denaturation in our assays may cause acute inflammatory stimulations leading to Arg1 expression. A similar phenomenon was also observed in human neutrophils, as heat inactivation did not impact neutrophil survival (S4*C*). This suggests that the major MDSC differentiating signal is not a protein.

Cancer cell–derived extracellular vesicles (EVs) serve as cargo for intercellular signaling and are heat labile (37–39). Thus, EVs can carry proteins, microRNAs, and even cell membrane–derived signaling molecules that may promote the activation and differentiation of neutrophils into MDSCs (37, 39). To test this possibility, we depleted more than 95% EVs from the KCKO culture supernatant (Fig. 4*D* and *SI Appendix*, S4*D*) (40). However,

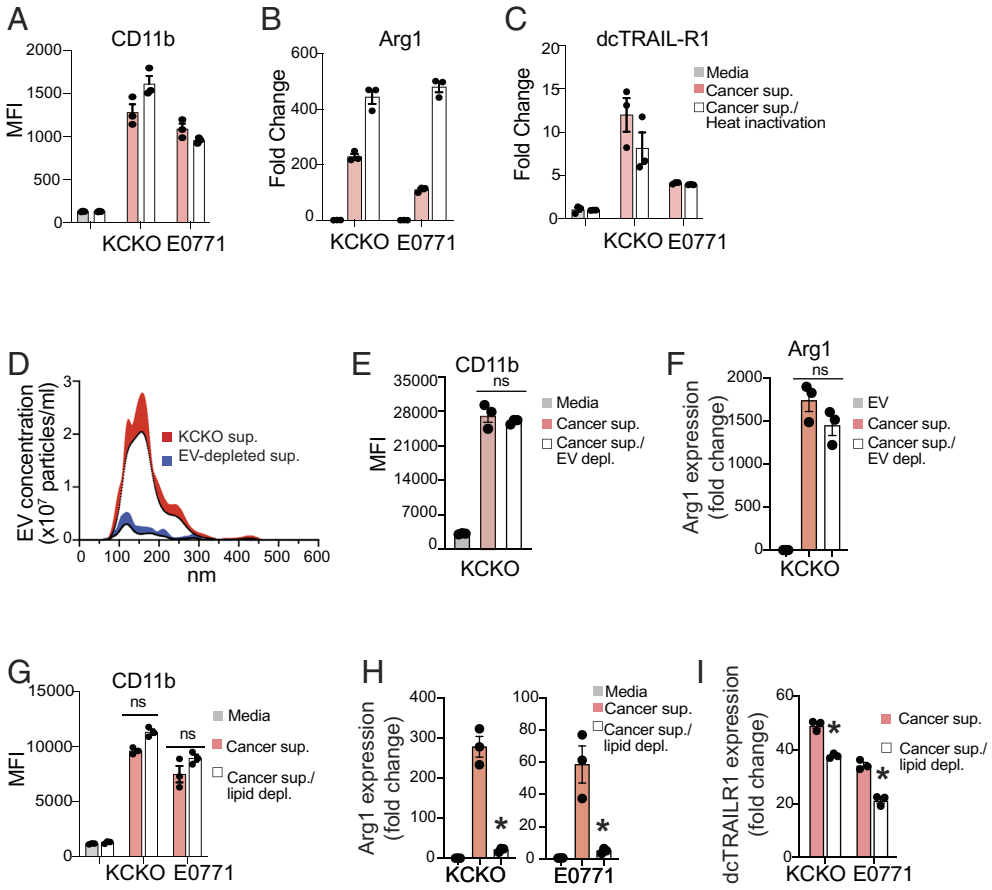

Fig. 4. Cancer-secreted lipid mediators induce PMN-MDSC differentiation in both murine and human cancers. (*A*–*C*) Neutrophil activation (*A*; CD11b MFI), Arg1 (*B*), and dcTrail-R1 (*C*) expression levels were quantified after overnight incubation in heat-inactivated KCKO cancer supernatant. (*D*) Mean and 95% CI of EV concentration in KCKO supernatant before and after EV depletion with ultracentrifugation. (*E* and *F*) Quantification of neutrophil activation (*E*) and Arg1 expression (*F*) after culturing with EV-depleted KCKO supernatant. (*G* and *H*) Neutrophil activation (*G*) and Arg1 expression (*H*) after incubation in lipid-depleted supernatants prepared from KCKO and E0771 murine cancers. (*I*) Expression of dcTrail-R1 in neutrophils after overnight coculture in lipid-depleted cancer supernatant. (*A*–*C*) One-way ANOVA test with Tukey's MCT, n = 3 (*A*) ns, (*B*) $P < 0.0001$, and (*C*) $P < 0.0001$. (*H* and *I*) Two-way ANOVA test, n = 3, $P < 0.0001$. (*E*–*G*) One-way ANOVA, Tukey's MCT, n = 3, ns.

depletion of EVs from cancer cell culture supernatant failed to inhibit MDSC differentiation, suggesting that EVs do not play a major role in this process (Fig. 4 *E* and *F*).

Next, we turned our focus to cancer-secreted lipid mediators, as many cancer-derived inflammatory mediators are heat-resistant lipid molecules (41, 42). To test this hypothesis, we selectively depleted lipids from the cancer cell supernatant using a lipid-binding micelle kit. Importantly, depletion of lipids did not change neutrophil activation (Fig. 4*G*) but drastically abrogated the ability of neutrophils to both survive in cancer supernatant and limited the ability of neutrophils to express the MDSC markers, including Arg1 and dcTrail-R1 across both murine and human cancers (Fig. 4 *H* and *I* and *SI Appendix*, S4 *E–F*). Importantly, the process of lipid depletion did not alter neutrophil survival or activation, suggesting that abrogation of MDSC phenotype is directly the result of depleted cancer secreted lipids (*SI Appendix*, S4 *G–H*).

Cancer-Secreted PAF Induces Neutrophil Differentiation. Given the conserved nature of lipid-mediated response across the array of murine and human cancers, we hypothesized that a common lipid molecule is likely responsible for neutrophil differentiation. To identify a key lipid mediator, we performed LC-MS lipidomic analyses of cancer-conditioned media prepared from murine KCKO and human PDAC3, HT29, H1299, and TOV11D cancer cell lines. Across the 5 different cancer types, we identified 4 conserved lipid molecules secreted by cancers: glucosylceramide (GlcCer; d18:1/16:0), ceramide-1-phosphate (Cer-1P; d18:1/16:0), platelet-activating factor (PAF; 1-*O*-alkyl-2-acetyl-*sn*-glycero-3-phosphocholine), and lysophosphatidylglycerol (LPG; 16:0) (Fig. 5 *A* and *B* and *SI Appendix*, S5*A*). Despite the established role of cancer-secreted PGE2 in MDSC differentiation, PGE2 metabolite, PGF2α, was only detected in KCKO and HT29 cancers, suggesting that other lipid mediators are also involved in MDSC differentiation (S5A). To determine whether any of these conserved lipids were sufficient to promote neutrophil differentiation, we directly added reconstituted lipids to cultured neutrophils and assayed Arg1 expression. As expected, adding all 4 lipids strongly induced Arg1 expression (Fig. 5*C*). Importantly, among these 4 lipids, PAF had the strongest effect on Arg1 and dcTrail-R1 expression (Fig. 5 *C–E*) and T cell suppression (Fig. 5*F*). ELISAs of the extracellular tumor interstitial fluid of orthotopic KCKO further confirmed the significant increase in PAF production in vivo (Fig. 5*G*). Consistently, a selective PAF receptor inhibitor, WEB-2086, abolished the neutrophil differentiation in both KCKO and E0771 cancer cell culture supernatants (Fig. 5*H*). Additionally, RNAseq of neutrophils pulsed with PAF for 24 h further highlighted significant upregulation of MDSC-associated gene signatures, highlighting the ability of PAF to promote MDSC differentiation similar to that observed in intratumoral neutrophils (26) (Fig. 5*I*).

LPCAT2 Expression Predicts Tumor Burden in PDAC Patients. LPCAT2 is the PAF-generating enzyme (43). To understand the role of PAF in human cancer, we analyzed TCGA and GTEx metagenomic datasets to investigate associations between LPCAT2 expression and cancer patient survival. Similar to our culture system results, we found that LPCAT2 is significantly up-regulated in PDAC patients compared to healthy controls (Fig. 6*A*). Additionally, patients with higher LPCAT2 expression had significantly worse clinical outcomes (Fig. 6*B*), which was associated with increased neutrophil infiltration within the tumor (Fig. 6*C*). Additionally, we observed a significant correlation between LPCAT2 expression in cancer and patient mortality across multiple cancer types, further suggesting a conserved nature of PAF-mediated immunosuppressive and neutrophil differentiation in human cancers (Fig. 6*D*). Consistent with these human patient data, inhibition of PAFR signaling with WEB2086 in multiple different PAF-producing mouse cancers, including KCKO, B16F0, and E0771 (S6A), significantly decreased tumor growth in vivo and dcTrail-R1 expression in intratumoral neutrophils without significant changes in tumor-associated neutrophil numbers (Fig. 6 *E–J* and *SI Appendix*, S6 *B–D*). Importantly, WEB2086 did not alter the cancer cell growth rate in vitro, suggesting its effect on cancer cell–extrinsic factors (S6*E*).

Discussion

The important function of myeloid cells in cancer formation was proposed as early as the 1960s when high levels of myeloid cell infiltrates were found to enhance tumor growth in tumor-bearing mice (44). Although we now better understand the immunomodulatory and cancer-promoting properties of myeloid cells, our knowledge of the mechanism involved in neutrophil recruitment, activation, and MDSC differentiation remains elusive due to the associated technical challenges of working with these fragile cell types (45). Neutrophils are difficult to culture and genetically manipulate without breeding germline mutations in mice, which quickly increases the time and cost associated with studying tumor-associated neutrophils. To overcome these challenges, we validated that ex vivo coculture systems of cancer cells and neutrophils recapitulate both transcriptional and phenotypic features of an immunosuppressive subset of intratumoral neutrophils, establishing a highly reproducible method for studying MDSC biology and the cancer secretome.

Using this approach, we demonstrated that among cancer-secreted proteins, EVs, and lipid molecules, only lipid-mediated signals functioned at physiological levels to promote neutrophil survival and MDSC differentiation in vitro. Most inflammatory lipids within mammalian systems are highly localized partly because of the associated short half-lives (46). Here, our findings highlight that cancer-derived lipid-mediated signals contribute to MDSC differentiation and are likely localized to or near the tumor site. Bioactive phospholipid mediators are integral for neutrophil recruitment and activation at sites of infection and injury (12). Our results highlight that multiple human and murine cancers rely on the same conserved lipid signals to promote the recruitment and activation of neutrophils. Paradoxically, chronic exposure to classically defined inflammatory molecules, such as PAF, can phenotypically reprogram neutrophils into immunosuppressive subsets (12, 13). This is likely a protective evolutionary mechanism to limit hyperinflammatory states and initiate the subsequent anti-inflammatory, wound-healing response. Cancers have been described as "wounds that do not heal" (47) and rely on the intricate balance between inflammation to recruit innate cells while simultaneously establishing an immunosuppressive environment to reduce adaptive immunity. Disruption of this intricate inflammatory balance can dramatically shift intratumoral immune composition and alter the trajectory of cancer growth. Our studies with an acute orthotopic KCKO murine PDAC model do not define the role of tumor-derived factors that may systemically regulate MDSC differentiation in other organs at different stages of tumors (22); nonetheless, cancer-secreted lipid signals localized near the tumor site may work in concert with other inflammatory mediators to control myeloid cell differentiation and ant-cancer host immunity.

Although the role of PAF in tumorigenesis is only in its infancy, few publications have highlighted similar tumor-promoting features of PAF in B16F10 and TC1 tumors (48–50). Tumors grown in PAFR knockout mice had drastically slower growth kinetics and decreased immunosuppressive immune cell composition.

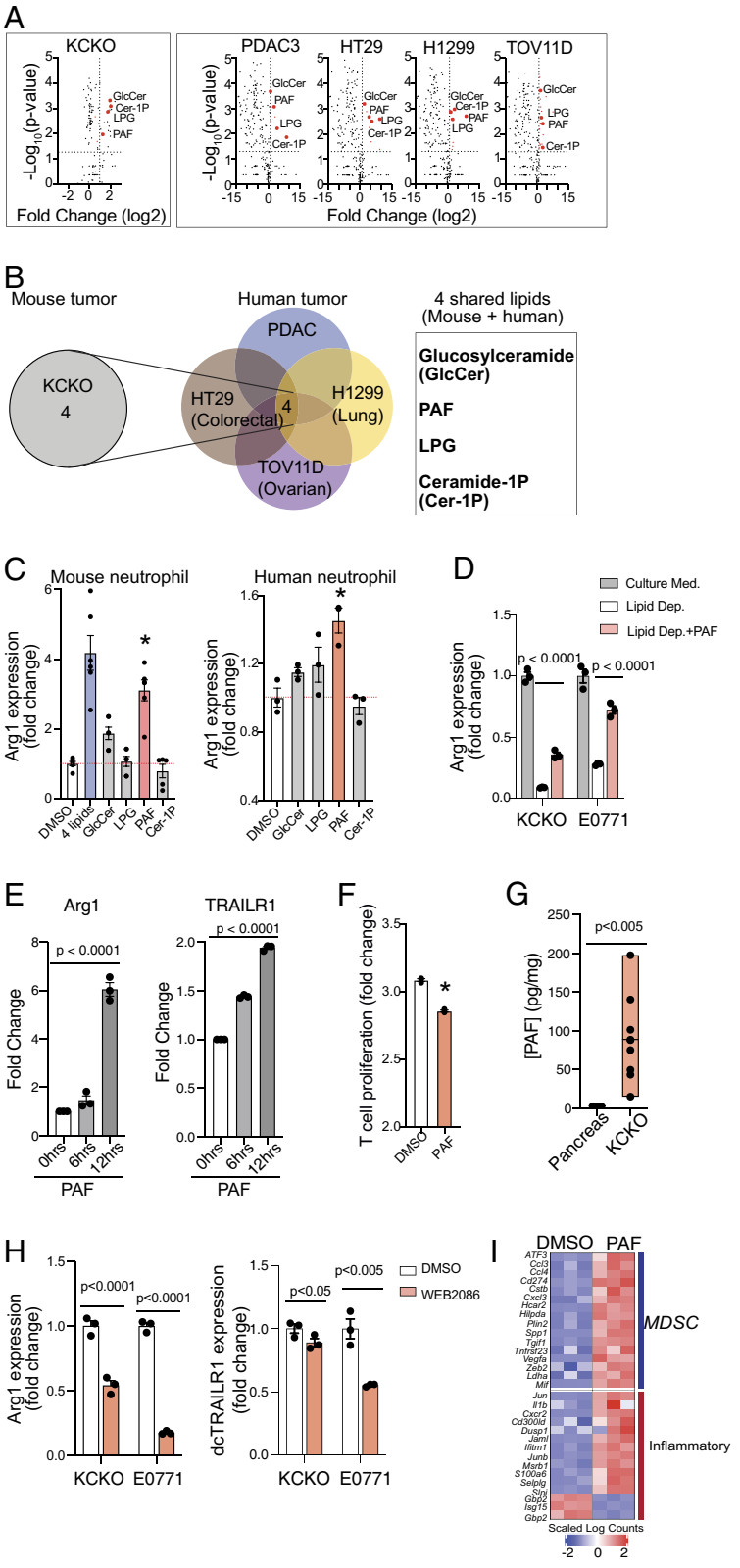

Fig. 5. Cancer-secreted PAF induces neutrophil differentiation. (*A*) LC-MS analysis of lipids present in KCKO, PDAC3, HT29, H1299, and TOV11D cancer supernatants. Lipids with FC > 2 and *P*-value < 0.05 are marked (red). (*B*) Four shared lipids are identified across murine and human cancers. (*C*) Arg1 expression in murine and human neutrophils after adding reconstituted lipids (1 μM) to media. (*D*) Arg1 expression in murine neutrophils after adding PAF to lipid-depleted KCKO and E0771 supernatant. (*E*) Kinetics of Arg1 and dcTrail-R1 expression in murine neutrophils in the presence of PAF. (*F*) CD8 T cell proliferation after overnight coculture with neutrophils conditioned with DMSO or PAF. (*G*) ELISA quantifying concentration of PAF in TIF of mock surgery (pancreas) vs. orthotopic KCKO tumors. (*H*) Quantification of Arg1 and dcTrail-R1 expression after incubation of neutrophils in KCKO and E0771 supernatants in the presence of PAFR inhibitor, WEB-2086 (5 μM). (*I*) Bulk RNAseq of neutrophils cultured in the presence of DMSO or PAF overnight, highlighting the expression of intratumoral MDSC and inflammatory signature genes. (*C* and *E*) One-way ANOVA, Tukey's MCT, n = 3, *P* < 0.05 and <0.0001, respectively. (*D*) Two-way ANOVA, Šidák MCT, n = 3, *P* < 0.0001. (*F* and *H*) Student's *t* test. n = 9 *P* < 0.005.

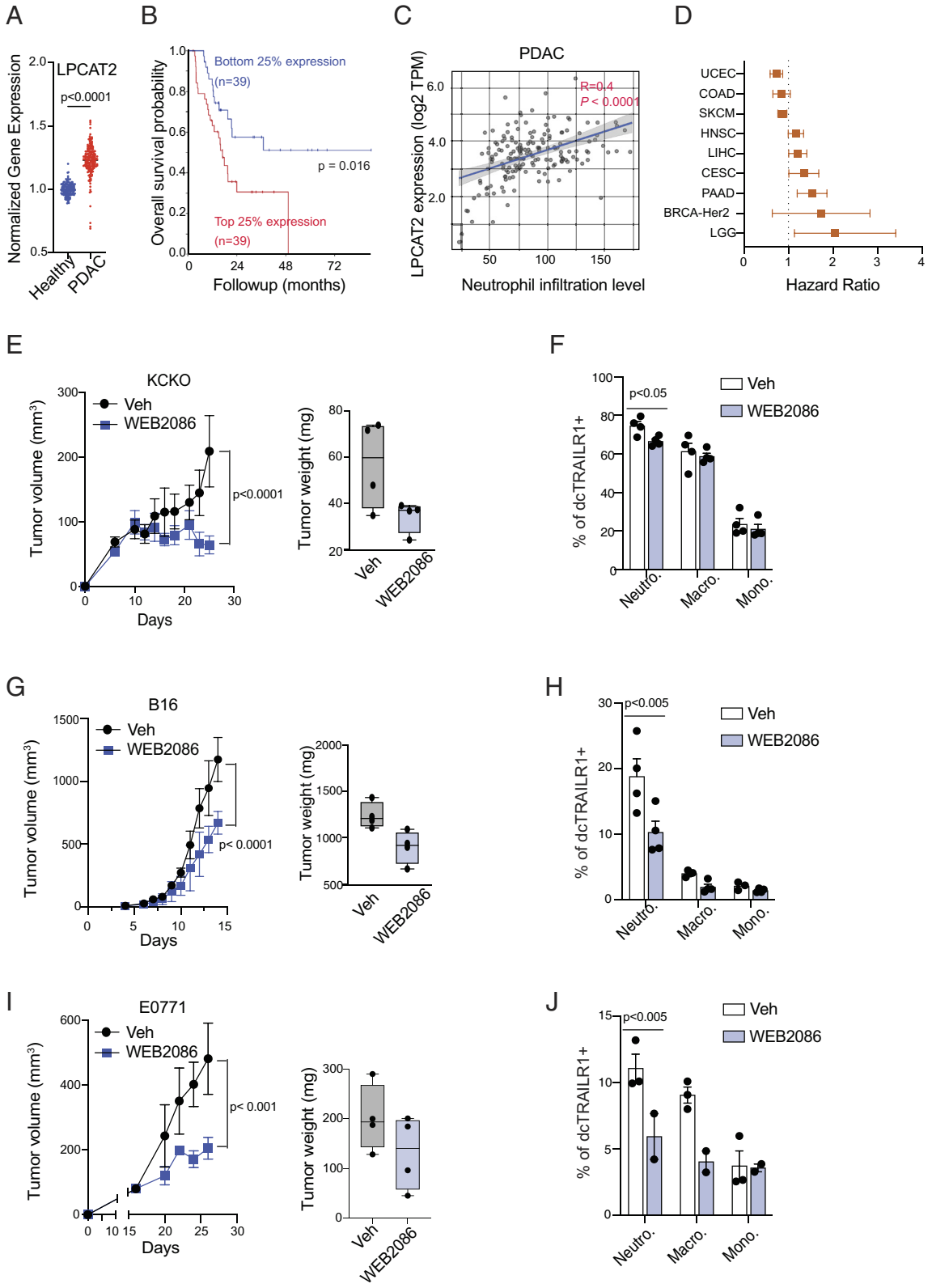

Fig. 6. Inhibition of PAFR limits tumor growth in vivo. (*A*) Normalized LPCAT2 expression in healthy pancreas vs. PDAC tumors was obtained using GTEX and TCGA datasets from the UCSC Xena data analysis tool. (*B*) TCGA survival curve subsetting top and bottom 25% LPCAT2 expressing PDAC tumors obtained using R2 Genome Browser tool. (*C*) Intratumoral neutrophil infiltration compared to LPCAT2 expression across human PDAC dataset obtained from TIMER 2.0 tool. (*D*) TCGA data correlating LPCAT2 expression and patient survival were obtained using the R2 genome browser tool. (*E*) KCKO cells growth kinetics and endpoint tumor weight at endpoint with vehicle (5% ethanol: PBS) and 10 mg/kg WEB2086. The drug was injected intraperitoneally (I.P.) every day. (*F*) dcTrail-R1 expression of tumor-infiltrating myeloid cells in vehicle vs. WEB2086-treated mice. (*G*) B16F0 growth kinetics and tumor weight and (*H*) expression of dcTrail-R1 in myeloid cells. (*I*) E0771 growth kinetics and tumor weight and (*J*) expression of dcTrail-R1 in myeloid cells. (*E*, *G*, *I*) Two-way ANOVA, n = 4. (*F*, *H*, *J*) Multiple *t* test, Holm–Šidák MCT, n = 4.

Our findings further corroborate that PAF secretion is highly conserved across many cancer types and targeting this pathway may alleviate the MDSC burden. However, further studies are still needed to investigate the inflammatory balance between PAF and other inflammatory and anti-inflammatory mediators within the TME.

Vastly heterogeneous cell types secrete a plethora of signaling molecules at the tumor microenvironment that can regulate immune cell differentiation both within the tumor as well as distal sites, including the spleen and the bone marrow, where they may function at physiological concentrations. However, our study primarily focuses on the direct impact of cancer-secreted factors on MDSC differentiation and does not define the importance of PAF in MDSC differentiation throughout the tumor life cycle, including during the initiation of cancer, after the establishment of an immunosuppressive TME or even at distal metastatic sites. Additionally, conversing signals between PAF and other inflammatory and anti-inflammatory factors may mediate different outcomes in neutrophils already present within a continuum of activation and differentiation status within the tumor microenvironment. Despite the limitation of the coculture system, we established a lipid-driven mechanism of MDSC differentiation that can directly alter cancer growth in vivo and may be implicated in human disease.

Materials and Methods

Antibodies and Reagents. Anti-mouse CD16/CD32 Fc blocker, Ly6G-V421 (1A8), CD11b-PE (M1/70), CD8-APC (53-6.7), CD4-FITC(RM4-5), CD45-APC-Cy7 (30-F11), AnnV-APC, and 7AAD were purchased from BioLegend. Cell Trace Violet, Cell Trace CFSE, and UltraComp eBeads were purchased from Invitrogen. Recombinant human ICAM1/CD54Fc Chimera Protein was purchased from R&D Biosystems. Bioactive lipids including PAF(22:5), Glu(β)Cer(d18:1/16:0), Cer-1-P(d18:1/24:1), and LPG(18:1) were purchased from Avanti Polar Lipids. WEB2086 was purchased from Tocris Bioscience. LC/MS lipidomic screen was performed by Human Metabolome Technologies, Inc. The PAF ELISA kit (ab287801) and cytokine array membranes (ab193659) were purchased from Abcam.

Mice. C57BL/6 J mice were purchased from Jackson Laboratory. The Catchup (Ly6G Cre/ROSAtdTomato) mouse line was a gift from M. Gunzer (51). All animal experiments were performed in the Association for Assessment and Accreditation of Laboratory Animal Care International–accredited, specific pathogen-free facilities in the Division of Laboratory Animal Resources of the University of Rochester Medical Center. All animal experiments were approved by the University Committee on Animal Resources at the University of Rochester.

Cell Culture. KCKO, MC38, E0771, and HT29 cell lines were purchased from ATCC. Human PDAC3 and CAF cancer and fibroblast cell lines were generous gifts from David Ting, as described previously (52, 53). H1299, TOV11D, and HT29 cancer cell lines were gifted by Darren Carpizzo. All cell lines were cultured in DMEM (Life Technologies) supplemented with 10% FBS, 1% antibiotic–antimycotic (Gibco), 2 mM L-glutamine (Gibco), 20 mM HEPES (Gibco), 1% MEM nonessential amino acids (Gibco), and 50 μM β-mercaptoethanol (Sigma-Aldrich).

Cancer Supernatant Preparation. Once cancer cells reached 60% confluency in a 10 cm dish, old culture medium was changed with 10 mL of fresh culture media, and the cells were allowed to grow for one day. After one day, the culture media was pipetted into a 15 mL conical and centrifuged at 2000×g for 10 min to remove any cell debris and additionally filtered through a 0.22 μm filter. Heat inactivation of culture media was achieved by placing the culture media in a 95 °C water bath for 10 min. The media was cooled to room temperature before culturing with neutrophils. To deplete lipids from cancer supernatant, we added Cleanascite reagent (Biotech Support Group) according to the manufacturer's protocol. Briefly, 1:4 ratio of Cleanascite reagent was added to culture media at room temperature and placed on a rocking platform. After 10 min, the media was centrifuged at 1000×g for 5 min. The supernatant was transferred to another tube and centrifuged to remove any residual Cleanascite reagent.

Neutrophil Isolation. Neutrophils were isolated from the bone marrow by first dissecting the femur and tibia and flushing out the cells from the bone marrow using a 2 mL syringe. Single-cell suspension was achieved after filtering the bone marrow isolate through a 70 μm cell strainer. Neutrophils were enriched using the MojoSort mouse neutrophil isolation kit (BioLegend) according to the manufacturer's protocol. Neutrophils from the spleen were isolated from either naïve or tumor-bearing mice and gently mashed through a 70 μm cell strainer. Anti-Ly-6G Microbeads (Miltenyi Biotec) were added to cell suspension and passed through MACS LC columns (Miltenyi Biotec) to capture neutrophils. The neutrophils were removed by gently plunging the LC columns. Neutrophils from tumors were isolated by first dissecting the tumor, manually disrupting, and digesting in collagenase/dispase (Roche) for 30 min at 37 °C. Digested tumor suspensions were filtered through a 70 μm strainer to remove any extracellular matrix components. A similar microbead method was used for the spleen to isolate intratumoral neutrophils. Human neutrophils were isolated from the blood of healthy donors using 1-Step Polymorphs (Fisher Scientific). Briefly, up to 6 mL of whole blood was added atop 2 mL of polymorph. The tubes were centrifuged at 500xg for 45 min. Granulocyte layer cells were isolated and washed in HBSS solution containing 10 mM HEPES and 0.1% BSA. To lyse any contaminating RBCs, 1 mL ultrapure water was used to resuspend pelleted neutrophils, and after 30 s, 10 mL of HBSS solution was added to the tube to equilibrate the tonicity. The neutrophils were resuspended in HBSS solution, yielding 99% pure neutrophil isolates.

Neutrophil Survival Assay. A total of 1×10^6 naive neutrophils were cultured in 12-well cell culture plates with 500 μL culture media or cancer supernatant. overnight. The next day, neutrophils were transferred to Eppendorf tubes and stained with Ly6G, Annexin V, or 7AAD to quantify the number and percentage of live and dead neutrophils using flow cytometry.

T Cell Isolation. Mouse CD8 T cells were isolated from the spleen and lymph nodes of C57BL/6 mice. The organs were gently mashed through a 70 μm cell strainer to resuspend single-cell suspension. CD8 T cells were enriched by magnetic-bead depletion with rat anti-mouse MHC II antibody (M5/114) and rat anti-mouse CD4 antibody (GK1.5), followed by sheep anti-rat IgG magnetic beads (Invitrogen 11035). The enriched CD8 T cells were either used in T cell proliferation assays or activated with plate-bound CD3e Ab (1 μg/mL) and CD28 Ab (1.6 μg/mL) in RPMI medium supplemented with 80 U/mL IL-2.

T Cell Proliferation Assay. Naive CD8 T cells were stained with Cell Trace CFSE at 1 μM concentration for 15 min. After staining, 5×10^5cells were added to a 24-well plate that was previously coated with CD3e (1 μg/mL) and CD28 (1.6 μg/mL) antibodies. For MDSC suppression assays, 1:1 ratio of CD8 T cells and naïve neutrophils or MDSCs were cocultured in RPMI medium containing 80 U/mL IL-2. After 2–3 d, the cells were pipetted, washed, and stained with CD8 antibody and analyzed with the BD LSR II flow cytometer for proliferation.

T Cell Cytotoxicity Assay. KCKO and E0771 cells were pulsed with 1 μg/mL OVA peptides for 20 min at 37 °C. After washing the cells with PBS, cancer cells were seeded in 24-well plates at 1×10^4 cells per well, and neutrophils that were cultured in cancer supernatant overnight and/or effector cells (OT-I T cells) were added to the target cells at a 10:1:1 ratio of cancer cells: neutrophils: CD8 T cells. After 24 h, 7-AAD dye was treated for 10 min, and cells were analyzed on a BD LSR II flow cytometer.

3D Tumoroid Assay. Tumor spheroids were generated as previously described (54). Briefly, AggreWell 800 culture plate (Stemcell) wells were pretreated with anti-adherence rinsing solution (Stemcell) and centrifuged at 1,200 RPM for 5 min. Wells were rinsed with media, and cancer cells were added to generate spheroids with 4,000 to 5,000 cells per micro-well and spun at 1,200 RPM for 5 min. After 24 h, the spheroids were collected by gentle pipetting and allowed to settle in a 1.4 mL Eppendorf tube, and excess media was aspirated. A total of 5×10^6 neutrophils were isolated from either the bone marrow or the spleen of catchup or GFP mouse and resuspended in 50 μL complete D10 culture media and mixed with tumor spheroids. A volume of 50 μL of Matrigel (Corning) was added to the neutrophil/spheroid mixture and mixed thoroughly. The total volume (100 μL) was transferred to the center of the ΔT-dish (Bioptechs) and incubated at 37 °C chamber and 5% CO_2 for 30 min to allow the gel to polymerize. Once

solidified, 1 mL of Leibovitz's media supplemented with 20 mg/mL glucose was added to the dish and live-imaging time-lapse microscopy was performed. Video microscopy was conducted using the TE2000-U microscope (Nikon) coupled to a CoolSNAP HQ CCD camera with a 10× objective and 0.45 numerical aperture. The ΔT-dish was maintained in a 37 °C chamber. Brightfield and fluorescent images were acquired every 2 min for up to 12 h. For quantification, a single region of interest (ROI) was drawn around the tumoroid, and the mean fluorescence intensity increase within the ROI over time for Catchup neutrophils was measured.

2D Migration Imaging. Migration analysis was performed in Volocity software (PerkinElmer). We excluded cells that are smaller than 10 μm and greater than 200 μm. Additionally, static cells were ignored, broken tracks were automatically joined, and cell tracks less than 20 μm were excluded. We also omitted neutrophils that were migrating for less than 5 min of the 20-min movie and removed cells that Volocity incorrectly tracked.

RT-qPCR. For gene expression analysis of mouse or human neutrophils, cells were lysed in RLT buffer, and RNA was isolated with the RNeasy plus mini kit (Qiagen) according to the manufacturer's instructions. After RNA concentration and purity were checked using a NanoDrop, 100 ng of RNA per reaction was subsequently converted to cDNA using the SuperScript VILO cDNA synthesis kit (Invitrogen). Samples were assayed using SsoAdvanced Universal SYBR Green Supermix (Bio-Rad), and PCR was performed on a CFX Connect real-time PCR detection system (Bio-Rad). Data were normalized to β-Actin. Relative transcript levels were analyzed using the cycling threshold ($2-\Delta\Delta CT$) method. The following primers were used, with the format "target (forward primer/reverse primer)": *Arg1* (CATTGGCTTGCGAGACGTAGAC/GCTGAAGGTCTCTTCCATCACC), *Actin* (CATTGCTGACAGGATGCAGAAGG/TGCTGGAAGGTGGACAGTGAGG), *Tnfrsf23* (TATGGTGGCTGACTGTTCTGCC/AGCTGTGGAGTTGCATTCCTGG), human_*ARG1* (GTTTCTCAAGCAGACCAGCC/GCTCAAGTGCAGCAAAGAGA), Actin(CACCATTGGCAAT GAGCGGTTC/AGGTCTTTGCGGATGTCCACGT).

RNA Sequencing. Total RNA from neutrophils was isolated using the RNeasy plus mini kit (Qiagen). Total RNA was preamplified with the SMARTer Ultra Low Input kit v4 per the manufacturer's protocol (Clontech). CDNA quality and quantity were measured using the Qubit fluorometer (Life Technologies) and Agilent Bioanalyzer 2100. CDNA was used to generate Illumina-compatible sequencing libraries using the NexteraXT library preparation kit (Illumina). The amplified libraries were hybridized to Illumina flow cell and sequenced using the NextSeq 550 sequencer (Illumina). Reads were aligned with STAR-2.7.0 and reads quantified with Subread-1.6.4. DESeq2-1.26.0 was used to normalize count matrix and assess differential expression with adjusted *P* value < 0.05. Heatmap was created using pheatmap (1.0.12) using DESeq2-normalized counts. Heat map representations were produced using RStudio (1.3.1093) and GraphPad Prism (v10).

Tumor Interstitial Fluid Isolation. TIF was isolated using the protocol detailed by Helge Wiig (55). Briefly, orthotopic tumors or pancreas mock injected with PBS were dissected from mice, flushed with PBS, and quickly blotted to remove visual blood. Since the tumors were large, they were sectioned into ~0.5 g pieces and placed in Spin-X 0.22 μm filter tubes (Costar) and centrifuged for 10 min at 100 xg. The flowthrough was immediately frozen at -80 °C until ready for analysis with ELISA. For direct neutrophil culture assays, the interstitial fluid was diluted 1:5 in culture media.

Statistical Analysis. All statistical tests were performed with GraphPad Prism (v10). Statistical analysis was performed using two-way ANOVA, ordinary one-way ANOVA with a Tukey's multiple-comparison post hoc test, an unpaired and paired *t* test, and a Mann–Whitney test when appropriate. Differences were considered significant when *P* values were <0.05. Data distribution was assumed to be normal, but this was not formally tested. All in vivo experiments were performed on C57BL/6 mice aged 6 to 12 wk old and both males and females. All experiments were performed with age and sex matched mice that were randomly assigned to each group. For the in vitro assays, samples and cell conditions were randomly distributed across treatment groups. For in vivo experiments, there was no blinding in collection and analysis of the experimental data due to requirements for cage labeling and staffing needs. For in vitro experiments, all the treatments were performed in a parallel manner without the risk of bias in interpretation. No data were excluded from the study.

Data, Materials, and Software Availability. Bulk RNA seq data Flow cytometry data LC-MS lipidomic data are available for download in Dryad (DOI: 10.5061/dryad.1rn8pk13d (56) and https://doi.org/10.5061/dryad.866t1g209 (57)). RNAseq data have been deposited in GEO Repository (GSE273979) (58).

ACKNOWLEDGMENTS. We thank Adam Geber, Stephanie Renner, and all members of the Kim Laboratory for their comments during the course of these studies and input during the preparation of the manuscript. We would like to thank Darren Carpizo and David Ting for generously providing us with cell lines and samples. This work was funded by NIH grant AI102851 (M.K.); NIH grant AI147362 (M.K.); NIH grant HL160723 (M.K.); and NIH grant T32 GM007356 (A.D.).

Author affiliations: [a]Department of Microbiology and Immunology, David H. Smith Center for Vaccine Biology and Immunology, University of Rochester, Rochester, NY; [b]Department of Pathology, University of Rochester Medical Center, Rochester, NY; [c]Department of Surgery, University of Rochester Medical Center, Rochester, NY; and [d]Wilmot Cancer Institute, University of Rochester Medical Center, Rochester, NY

1. F. Veglia, M. Perego, D. Gabrilovich, Myeloid-derived suppressor cells coming of age. *Nat. Immunol.* **19**, 108–119 (2018).
2. L. Jin, H. S. Kim, J. Shi, Neutrophil in the pancreatic tumor microenvironment. *Biomolecules* **11**, 1170 (2021).
3. A. J. Gentles *et al.*, The prognostic landscape of genes and infiltrating immune cells across human cancers. *Nat. Med.* **21**, 938–945 (2015).
4. L. A. Pekarek, B. A. Starr, A. Y. Toledano, H. Schreiber, Inhibition of tumor growth by elimination of granulocytes. *J. Exp. Med.* **181**, 435–440 (1995).
5. R. F. Gabitass, N. E. Annels, D. D. Stocken, H. A. Pandha, G. W. Middleton, Elevated myeloid-derived suppressor cells in pancreatic, esophageal and gastric cancer are an independent prognostic factor and are associated with significant elevation of the Th2 cytokine interleukin-13. *Cancer Immunol. Immunother* **60**, 1419–1430 (2011).
6. Y. Wang *et al.*, Neutrophils infiltrating pancreatic ductal adenocarcinoma indicate higher malignancy and worse prognosis. *Biochem. Biophys. Res. Commun.* **501**, 313–319 (2018).
7. M. E. Shaul, Z. G. Fridlender, Tumour-associated neutrophils in patients with cancer. *Nat. Rev. Clin. Oncol.* **16**, 601–620 (2019).
8. C. W. Steele *et al.*, CXCR2 inhibition profoundly suppresses metastases and augments immunotherapy in pancreatic ductal adenocarcinoma. *Cancer Cell* **29**, 832–845 (2016).
9. L. Yang *et al.*, Abrogation of TGF beta signaling in mammary carcinomas recruits Gr-1+CD11b+ myeloid cells that promote metastasis. *Cancer Cell* **13**, 23–35 (2008).
10. S. K. Bunt, V. K. Clements, E. M. Hanson, P. Sinha, S. Ostrand-Rosenberg, Inflammation enhances myeloid-derived suppressor cell cross-talk by signaling through Toll-like receptor 4. *J. Leukoc. Biol.* **85**, 996–1004 (2009).
11. S. K. Bunt, P. Sinha, V. K. Clements, J. Leips, S. Ostrand-Rosenberg, Inflammation induces myeloid-derived suppressor cells that facilitate tumor progression. *J. Immunol.* **176**, 284–290 (2006).
12. E. Ricciotti, G. A. FitzGerald, Prostaglandins and inflammation. *Arterioscler Thromb. Vasc. Biol.* **31**, 986–1000 (2011).
13. C. A. Loynes *et al.*, PGE(2) production at sites of tissue injury promotes an anti-inflammatory neutrophil phenotype and determines the outcome of inflammation resolution in vivo. *Sci. Adv.* **4**, eaar8320 (2018).
14. A. Greenhough *et al.*, The COX-2/PGE2 pathway: Key roles in the hallmarks of cancer and adaptation to the tumour microenvironment. *Carcinogenesis* **30**, 377–386 (2009).
15. F. R. Khuri *et al.*, Cyclooxygenase-2 overexpression is a marker of poor prognosis in stage I non-small cell lung cancer. *Clin. Cancer Res.* **7**, 861–867 (2001).
16. H. Matsubayashi *et al.*, Tumor COX-2 expression and prognosis of patients with resectable pancreatic cancer. *Cancer Biol. Ther.* **6**, 1569–1575 (2007).
17. K. C. Corn, M. A. Windham, M. Rafat, Lipids in the tumor microenvironment: From cancer progression to treatment. *Prog. Lipid Res.* **80**, 101055 (2020).
18. M. Zheng *et al.*, The impact of lipids on the cancer-immunity cycle and strategies for modulating lipid metabolism to improve cancer immunotherapy. *Acta Pharm. Sin B.* **13**, 1488–1497 (2023).
19. D. Thumkeo *et al.*, PGE(2)-EP2/EP4 signaling elicits immunosuppression by driving the mregDC-Treg axis in inflammatory tumor microenvironment. *Cell Rep.* **39**, 110914 (2022).
20. H. Zhang *et al.*, Annexin A2/TLR2/MYD88 pathway induces arginase 1 expression in tumor-associated neutrophils. *J. Clin. Invest.* **132** (2022).
21. G. Di Conza *et al.*, Tumor-induced reshuffling of lipid composition on the endoplasmic reticulum membrane sustains macrophage survival and pro-tumorigenic activity. *Nat. Immunol.* **22**, 1403–1415 (2021).
22. A. Kidiyoor *et al.*, Pancreatic cancer cells isolated from Muc1-null tumors favor the generation of a mature less suppressive MDSC population. *Front. Immunol.* **5**, 67 (2014).
23. G. Werba *et al.*, Single-cell RNA sequencing reveals the effects of chemotherapy on human pancreatic adenocarcinoma and its tumor microenvironment. *Nat. Commun.* **14**, 797 (2023).
24. L. Wang *et al.*, Single-cell RNA-seq analysis reveals BHLHE40-driven pro-tumour neutrophils with hyperactivated glycolysis in pancreatic tumour microenvironment. *Gut* **72**, 958–971 (2023).
25. R. R. Maas *et al.*, The local microenvironment drives activation of neutrophils in human brain tumors. *Cell* **186**, 4546–4566.e27 (2023).
26. M. S. F. Ng *et al.*, Deterministic reprogramming of neutrophils within tumors. *Science* **383**, eadf6493 (2024).
27. P. C. Rodriguez *et al.*, Arginase I production in the tumor microenvironment by mature myeloid cells inhibits T-cell receptor expression and antigen-specific T-cell responses. *Cancer Res.* **64**, 5839–5849 (2004).

28. M. Munder *et al.*, Suppression of T-cell functions by human granulocyte arginase. *Blood* **108**, 1627–1634 (2006).
29. H. Sengelov, L. Kjeldsen, M. S. Diamond, T. A. Springer, N. Borregaard, Subcellular localization and dynamics of Mac-1 (alpha m beta 2) in human neutrophils. *J. Clin. Invest.* **92**, 1467–1476 (1993).
30. D. B. Kuhns, D. A. Long Priel, J. I. Gallin, Loss of L-selectin (CD62L) on human neutrophils following exudation in vivo. *Cell Immunol.* **164**, 306–310 (1995).
31. X. Su *et al.*, Breast cancer-derived GM-CSF regulates arginase 1 in myeloid cells to promote an immunosuppressive microenvironment. *J. Clin. Invest.* **131** (2021).
32. H. Liu *et al.*, Blocking iASPP/Nrf2/M-CSF axis improves anti-cancer effect of chemotherapy-induced senescence by attenuating M2 polarization. *Cell Death Dis.* **13**, 166 (2022).
33. M. Kowanetz *et al.*, Granulocyte-colony stimulating factor promotes lung metastasis through mobilization of Ly6G+Ly6C+ granulocytes. *Proc. Natl. Acad. Sci. U.S.A.* **107**, 21248–21255 (2010).
34. W. C. Lee, P. Y. Hsu, H. Y. Hsu, Stem cell factor produced by tumor cells expands myeloid-derived suppressor cells in mice. *Sci. Rep.* **10**, 11257 (2020).
35. R. D. Soltis, D. Hasz, M. J. Morris, I. D. Wilson, The effect of heat inactivation of serum on aggregation of immunoglobulins. *Immunology* **36**, 37–45 (1979).
36. L. Saso *et al.*, Inhibition of heat-induced denaturation of albumin by nonsteroidal antiinflammatory drugs (NSAIDs): Pharmacological implications. *Arch. Pharm. Res.* **24**, 150–158 (2001).
37. E. Yang *et al.*, Exosome-mediated metabolic reprogramming: The emerging role in tumor microenvironment remodeling and its influence on cancer progression. *Signal Transduct Target Ther.* **5**, 242 (2020).
38. E. Schulz, A. Karagianni, M. Koch, G. Fuhrmann, Hot EVs – How temperature affects extracellular vesicles. *Eur. J. Pharm. Biopharm.* **146**, 55–63 (2020).
39. P. Penfornis, K. C. Vallabhaneni, J. Whitt, R. Pochampally, Extracellular vesicles as carriers of microRNA, proteins and lipids in tumor microenvironment. *Int. J. Cancer* **138**, 14–21 (2016).
40. Z. Andreu, M. Yanez-Mo, Tetraspanins in extracellular vesicle formation and function. *Front. Immunol.* **5**, 442 (2014).
41. M. Bennett, D. W. Gilroy, Lipid mediators in inflammation. *Microbiol. Spectr.* **4**, 21 (2016).
42. C. N. Serhan, N. Chiang, T. E. Van Dyke, Resolving inflammation: Dual anti-inflammatory and pro-resolution lipid mediators. *Nat. Rev. Immunol.* **8**, 349–361 (2008).
43. H. Shindou *et al.*, A single enzyme catalyzes both platelet-activating factor production and membrane biogenesis of inflammatory cells. Cloning and characterization of acetyl-CoA:LYSO-PAF acetyltransferase. *J. Biol. Chem.* **282**, 6532–6539 (2007).
44. E. J. Lappat, M. Cawein, A study of the leukemoid response to transplantable a-280 tumor in mice. *Cancer Res.* **24**, 302–311 (1964).
45. T. N. Mayadas, X. Cullere, C. A. Lowell, The multifaceted functions of neutrophils. *Annu. Rev. Pathol.* **9**, 181–218 (2014).
46. H. Tesch, W. Konig, Origin and biological role of lipid mediators during inflammation (author's transl). *Immun. Infekt* **7**, 157–164 (1979).
47. H. F. Dvorak, Tumors: Wounds that do not heal. Similarities between tumor stroma generation and wound healing. N Engl. *J. Med.* **315**, 1650–1659 (1986).
48. I. A. da Silva Junior, S. C. Stone, R. M. Rossetti, S. Jancar, A. P. Lepique, Modulation of tumor-associated macrophages (TAM) Phenotype by platelet-activating factor (PAF). *Receptor. J. Immunol. Res.* **2017**, 5482768 (2017).
49. A. C. Onuchic *et al.*, Expression of PAFR as part of a prosurvival response to chemotherapy: A novel target for combination therapy in melanoma. *Mediators Inflamm.* **2012**, 175408 (2012).
50. R. P. Sahu *et al.*, The environmental stressor ultraviolet B radiation inhibits murine antitumor immunity through its ability to generate platelet-activating factor agonists. *Carcinogenesis* **33**, 1360–1367 (2012).
51. A. Hasenberg *et al.*, Catchup: A mouse model for imaging-based tracking and modulation of neutrophil granulocytes. *Nat. Methods* **12**, 445–452 (2015).
52. M. Ligorio *et al.*, Stromal microenvironment shapes the intratumoral architecture of pancreatic cancer. *Cell* **178**, 160–175.e27 (2019).
53. R. L. Porter *et al.*, Epithelial to mesenchymal plasticity and differential response to therapies in pancreatic ductal adenocarcinoma. *Proc. Natl. Acad. Sci. U.S.A.* **116**, 26835–26845 (2019).
54. C. J. Sailer *et al.*, PD-1(Hi) CAR-T cells provide superior protection against solid tumors. *Front. Immunol.* **14**, 1187850 (2023).
55. H. Haslene-Hox *et al.*, A new method for isolation of interstitial fluid from human solid tumors applied to proteomic analysis of ovarian carcinoma tissue. *PLoS ONE* **6**, e19217 (2011).
56. A. Dahal *et al.*, Platelet activating factor (PAF) promotes immunosuppressive neutrophil differentiation within tumors LC-MS Lipidomic Data set. Dryad. https://doi.org/10.5061/dryad.1rn8pk13d. Deposited 7 August 2024.
57. A. Dahal *et al.*, Platelet activating factor (PAF) promotes immunosuppressive neutrophil differentiation within tumors. Flow Cytometric Data set. https://doi.org/10.5061/dryad.866t1g209. Deposited 7 August 2024.
58. A. Dahal *et al.*, Platelet activating factor (PAF) promotes immunosuppressive neutrophil differentiation within tumors. NCBI GEO. https://www.ncbi.nlm.nih.gov/geo/query/acc.cgi?acc=GSE273979. Deposited 5 August 2024.